ADVANCED FUNCTIONAL MATERIALS
www.afm-journal.de

A Coenzyme-Based Deep Eutectic Supramolecular Polymer Bioadhesive

*Chunyan Cui, Yage Sun, Xiongfeng Nie, Xuxuan Yang, Fushuo Wang, and Wenguang Liu**

α-lipoic acid (LA), a coenzyme, has proved to have excellent antioxidant and antibacterial activities; however, its intrinsic hydrophobicity and metastability of polyLA remains a major challenge for the application of LA-based bulk materials in biomedical field. Herein, a self-stabilized LA-based deep eutectic supramolecular polymer (LA-DESP) adhesive is created by one-step heating the mixture of LA and sodium α-lipoate (LA-Na) (S-, R-isomer, racemate) without introducing any exogenous stabilizing molecules. The underlying deep eutectic effect in LA/LA-Na is unveiled to be originated from the multiple hydrogen bonds between polyLA and polyLA-Na, which not only prevent polyLA depolymerization but also lower the melting point of LA-DESP to the near body and pathological temperature. Copolymerization of LA and LA-Na slows down the dissociation of polyLA-Na, thus affording sustainable release of bioactive LA-based small molecules and satisfactory antioxidant and antibacterial functions. Also, the LA-DESP exhibits fast and tough adhesion to diverse substrates, including wet tissues, relying on its in situ curing property and rich carboxyl groups. The LA-DESP is explored as a tissue sealant, which can well replace surgical suture to enhance the wound healing of skin incision in a rat model. The unprecedented deep eutectic effect will provide a new strategy for the development of LA-based bioadhesives.

1. Introduction

Deep eutectic solvent (DES) is a new type of functional liquid with bright application prospects in various fields.[1] In general, DES comprises of a combination of hydrogen-bonded donor and a hydrogen-bonded acceptor with lower melting point as compared to either of its components by forming strong hydrogen bond interactions.[2] In recent years, DESs have gained momentum because of their low cost and green fabrication technique.[3] Nevertheless, most of the reported DESs have been developed as eco-friendly media. Although several studies have been conducted to introduce polymerizable monomer into DES to prepare bulk materials by secondary initiation polymerization, the obtained DES-based materials are not water resistant and can dissociate quickly to release small toxic molecules when used in wet environment. This will significantly limit the application of DES-based materials in the biomedical field.[4–6] Based on the basic principle of supramolecular polymerization, DES is also a typical hydrogen bond-driven supramolecular polymerization system.[7–9] Therefore, direct conversion of DES into supramolecular polymer materials in bulk without the introduction of secondary polymerization portends a new development direction of DES. By combining supramolecular polymerization with DES, Dong et al. developed a DES-based supramolecular polymer hot melt adhesive via the multiple hydrogen bonding interaction between cyclodextrin and natural acid, but the hot melt temperature of the formed adhesive was 80 °C, much higher than the body temperature. Thus, it still remains challenging to develop a DES adhesive suitable for in vivo application.[10]

α-Lipoic acid (LA), a natural endogenous bio-based small molecule in organisms, participates in mitochondrial activity and regulates energy metabolism.[11–13] Since the two adjacent sulfur atoms in its heterocyclic ring repel each other at a high electron cloud density, LA shows a strong reductive property and is considered to be an "omnipotent antioxidant" in redox reaction in human body.[11] Because of its unique biological activity and structural characteristics, LA has been widely applied in nanomedicine for the treatment of diabetes, Alzheimer's disease, and cancer.[14–17] Recently, the dynamic disulfide bond and the dynamic hydrogen bond between the terminal carboxyl group of LA were harnessed to construct supramolecular polymer networks in the form of hierarchical self-assembly.[18,19] However, the as-prepared polyLA was metastable due to the inverse closed-loop depolymerization initiated by terminal sulfur radicals.[20] Although polyLA-based supramolecular polymers can be stabilized by introducing multiple double-bond monomers, metal ions, and ionic liquids into the system, the resultant polyLA-based polymers are difficult to be purified, and the unreacted exogenous small molecules cannot be removed, posing a biosafety concern.[21–23] In addition, LA active molecules cannot effectively be released out from polyLA-based materials due to the high cross-linking density of polyLA and the intrinsic hydrophobicity of LA molecules, thereby sacrificing the biological activity of LA, such as antioxidant and antibacterial.[11,24,25] Although the abundant adhesive carboxyl

C. Cui, Y. Sun, X. Nie, X. Yang, F. Wang, W. Liu
School of Material Science and Engineering
Tianjin Key Laboratory of Composite and Functional Materials
Tianjin University
Tianjin 300352, China
E-mail: wgliu@tju.edu.cn

The ORCID identification number(s) for the author(s) of this article can be found under https://doi.org/10.1002/adfm.202307543

DOI: 10.1002/adfm.202307543

groups on the side chains afford the polyLA-based supramolecular polymers with robust tissue adhesion, the unavoidable release of foreign small molecules and high melting temperature (>70 °C) limit their application in vivo.[20,26]

The thermally initiated ring-opening self-polymerization of LA is reminiscent of deep eutectic effect, which benefits from the multiple hydrogen bonding interaction of the carboxyl groups at the end of LA, but the melt polymerization temperature is too high to be applied in vivo. In the experiment, we found that the ring opening polymerization of LA salt could not proceed by even heating to 200 °C, as shown in Figure S1 (Supporting Information). In LA salt, hydrogen bonds between carboxyls were broken, implying the H-bonding interactions are vital for ring-opening polymerization of LA. In light of the strong electron withdrawal property of —COO^- and its stronger hydrogen bonding interaction with —COOH compared with the two —COOH,[27,28] and supramolecular polymerization mechanism, and also taking into account introducing no exogenous small molecules, we hypothesize that employing hydrogen bond interaction between LA and LA salt may generate a novel biocompatible LA/LA-Na deep eutectic system with melting temperature near physiological temperature. Owing to adhesive capability of carboxyl, we envision that a LA-based deep eutectic supramolecular polymer (**LA-DESP**) adhesive could be created by simply heating the mixture of LA and LA salt (LA-Na was used in this work). In addition, the copolymerization between LA-Na and LA as well as the multiple hydrogen bonding interactions between —COO^- and —COOH could be expected to effectively quench the sulfur-free radicals at the end of polyLA and reduce the overall potential energy of the system,[22] thus resulting in a stable **LA-DESP** structure. Importantly, LA-Na active small molecules could be effectively released out from **LA-DESP** when it is used in a water or wet environment, due to the high hydrophilicity of LA-Na, signifying that this **LA-DESP** could be developed as an antioxidant and antibacterial bioglue for accelerating wound healing (**Figure 1**).

2. Results and Discussion

2.1. Preparation and Characterization of LA-DESPs

In this study, **LA-DESP**s were prepared simply by mixing LA with LA-Na in different mass ratios and then heating at different temperatures without further treatment (Here, S-isomer lipoic acid was selected for the following test. Unless otherwise specified, LA stands for S-isomer lipoic acid). As shown in **Figure 2**a and Figure S1 (Supporting Information), a series of light yellow viscous liquids of LA/LA-Na mixtures with different mass ratios were rapidly formed after being heated to different temperature. The thermal performances of LA, LA-Na, and LA/LA-Na mixtures were measured by differential scanning calorimetry (DSC) (Figure S2, Supporting Information). The results show that the melting point (T_m) of pristine LA powder was ≈65 °C, but after the deprotonation of LA to destroy the hydrogen bond between carboxyl groups, LA-Na could not be melted even heated to 200 °C, proving that formation of multiple hydrogen bond interactions was critical for the melting of LA. Interestingly, the melting points of the LA/LA-Na systems decreased significantly with increasing addition of LA into LA-Na (Figure 2b). When the ratio of LA to LA-Na was 0.5, the melting point of the mixture was ≈180 °C but dropped to 49.6 °C with further increasing LA/LA-Na ratio to 2, mirroring a typical eutectic phenomenon. When LA/LA-Na ratio was 3, the melting point of the system was reduced to 42.3 °C, much lower than that of pristine LA and LA-Na. Rheological tests also verified the formation of a deep eutectic system between LA and LA-Na (Figures S3 and S4, Supporting Information). The powder mixtures of LA and LA-Na with different mass ratios were pressed into compact flakes and rheological tests were carried out. Before reaching the melting point, the mixture was in a solid state, showing that G' was larger than G''. When the material was melted, it changed from a solid state to a viscous liquid state with G' less than G''. Therefore, the intersection points of G' and G'' corresponded to the melting points of LA/LA-Na mixture. Due to the thermal-initiated supramolecular self-assembly property of the LA-based monomer, the LA/LA-Na systems could be converted into supramolecular polymers after melting, and the obtained supramolecular polymer was named as **LA-DESP-x**, where **x** represented the mass ratio of LA to LA-Na (When LA/LA-Na was 0.5, the viscosity of the mixture was too high after melting and solidified immediately when it was cooled down, so it is difficult to prepare uniform samples. Therefore, the performances of **LA-DESP**$_{-0.5}$ were not investigated in this work).

The formation mechanism of the deep eutectic system between LA and LA-Na was first investigated by Fourier transform infrared spectroscopy (FT-IR). The —OH peak at 1249 cm^{-1} on the carboxyl group disappeared in the LA-Na structure, and the —C═O peak shifted from 1700 to 1545 cm^{-1}, suggesting that all carboxyl groups in LA-Na were deprotonated, that is, hydrogen bonds were disrupted.[29] As mentioned above, the pristine LA-Na still remained solid state at high temperature. While the appearance of the -OH peak at 1249 cm^{-1} in **LA-EDSP**s suggests the presence of —COOH in the LA/LA-Na binary system. Moreover, the —C═O peak on the carboxylate in **LA-EDSP**s exhibited an obvious red shift toward that of the pristine LA-Na monomer (Figure 2c,d), which means that strong hydrogen bond interaction between —COOH in LA structure and —COO^- in LA-Na structure occurred.[29] To further confirm the formation mechanism of deep eutectic effect, molecular dynamics simulation was performed to compare the strength of hydrogen bond formed between LA dimer and the hydrogen bond formed between LA and LA-Na. The results show that the bond energy of the hydrogen bond between LA dimer was −20.64 kcal mol^{-1}, while the bond energy of the hydrogen bond between LA and LA-Na was −44.3 kcal mol^{-1}, indicating that the hydrogen bond between LA and LA-Na (—COOH…O═C—O^-) was stronger than the hydrogen bond between LA dimer (—COOH…HOOC—) though the latter could form two hydrogen bonds (Figure 2e). This means that the formation of deep eutectic LA/LA-Na system was attributed to the multiple hydrogen bonds of —COOH…HOOC— and —COOH…O═C—O^-, in which the hydrogen bond of —COOH…O═C—O^- played a dominant role. Therefore, the melting points of **LA-DESP**s could be modulated to body temperature and pathological temperature by adjusting the ratio of LA to LA-Na, which overcomes the shortcoming of traditional LA-based hot melt adhesive that cannot be used in biomedical field because of their high melting point.

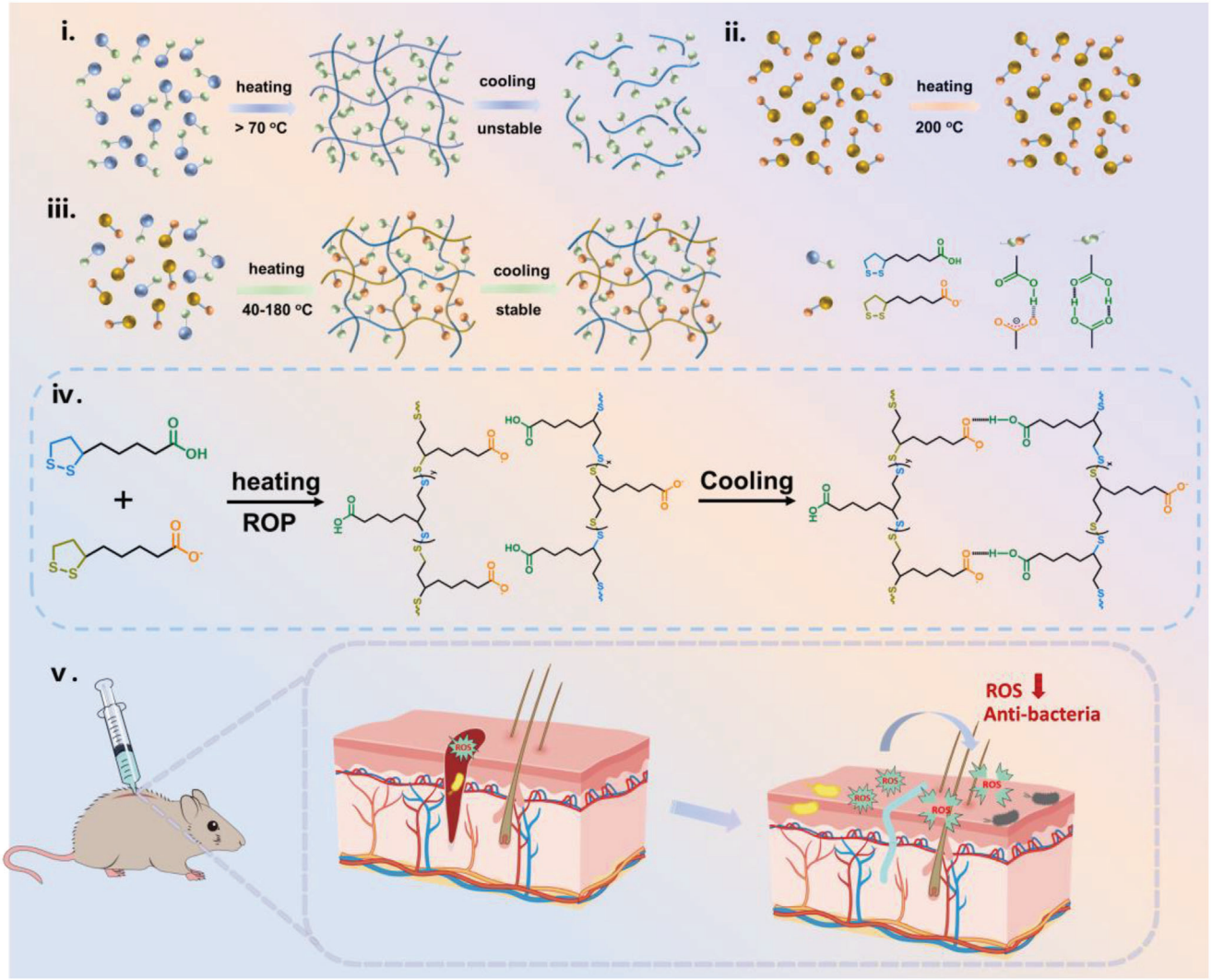

Figure 1. i) Preparation process and structural characteristics of polyLA; ii)Thermal stability of LA-Na; iii) Schematic diagram of preparation process and stabilization mechanism of LA-DESPs; iv) Chemical structure of LA-DESPs; v) Illustration of the LA-SEAP adhesive used for promoting skin wound healing.

The macroscopic photos of **LA-DESP**s in different states (Figure S1, Supporting Information) display that the pristine polyLA was unstable, and it was depolymerized into oligomers when cooled down to room temperature, while **LA-DESP**$_{-0.5}$, **LA-DESP**$_{-1}$, **LA-DESP**$_{-1.5}$, and **LA-DESP**$_{-2}$ could remain stable at room temperature. The reason is that the random copolymerization between LA-Na and LA could effectively quench the sulfur-free radicals at the end of polyLA, and the strong hydrogen bond of —COOH…O═C—O^{-} further reduced the potential energy of the system. However, when LA/LA-Na ratio was greater than 2, the **LA-EDSP** became unstable again when cooled down to room temperature. In this case, the content of LA was dominant, LA-Na in the system was insufficient to stabilize all polyLA, so partial polyLA in the system was depolymerized. The successful ROP of LA and LA-Na in the deep eutectic binary system was confirmed from the splitting of the characteristic Raman peak at 511 cm^{-1} ascribed to disulfide bonds in the five-membered ring into two peaks at 493 and 515 cm^{-1},[22,26,30] when LA/LA-Na ratios were 1 and 2, indicating that **LA-DESP**$_{-1}$ and **LA-DESP**$_{-2}$ were stable at room temperature. But for pure PolyLA and **LA-DESP**$_{-3}$, the characteristic Raman peak at 511 cm^{-1} for disulfide bonds in the five-membered ring was broadened rather than split, hinting that pure PolyLA and partial polyLA in **LA-DESP**$_{-3}$ was depolymerized after be cooled down to room temperature, which was consistent with the results of macroscopic photos (Figure 2f). The formation of stable copolymer of **LA-DESP** can also be confirmed by broadening of the peaks in the ^{1}H NMR spectra and obvious MS signal in a larger m/z range (Figures S5 and S6, Supporting Information). X-ray diffraction (XRD) was also employed to illustrate structural changes of the **LA-DESP**s with different ratios. Figure 2g shows that a diffraction peak in the small angle regime (<20°) appears in **LA-DESP**$_{-1}$, suggesting that there was a small amount of highly ordered nanoscale crystal structure in **LA-DESP**$_{-1}$, which was due to organized hierarchical

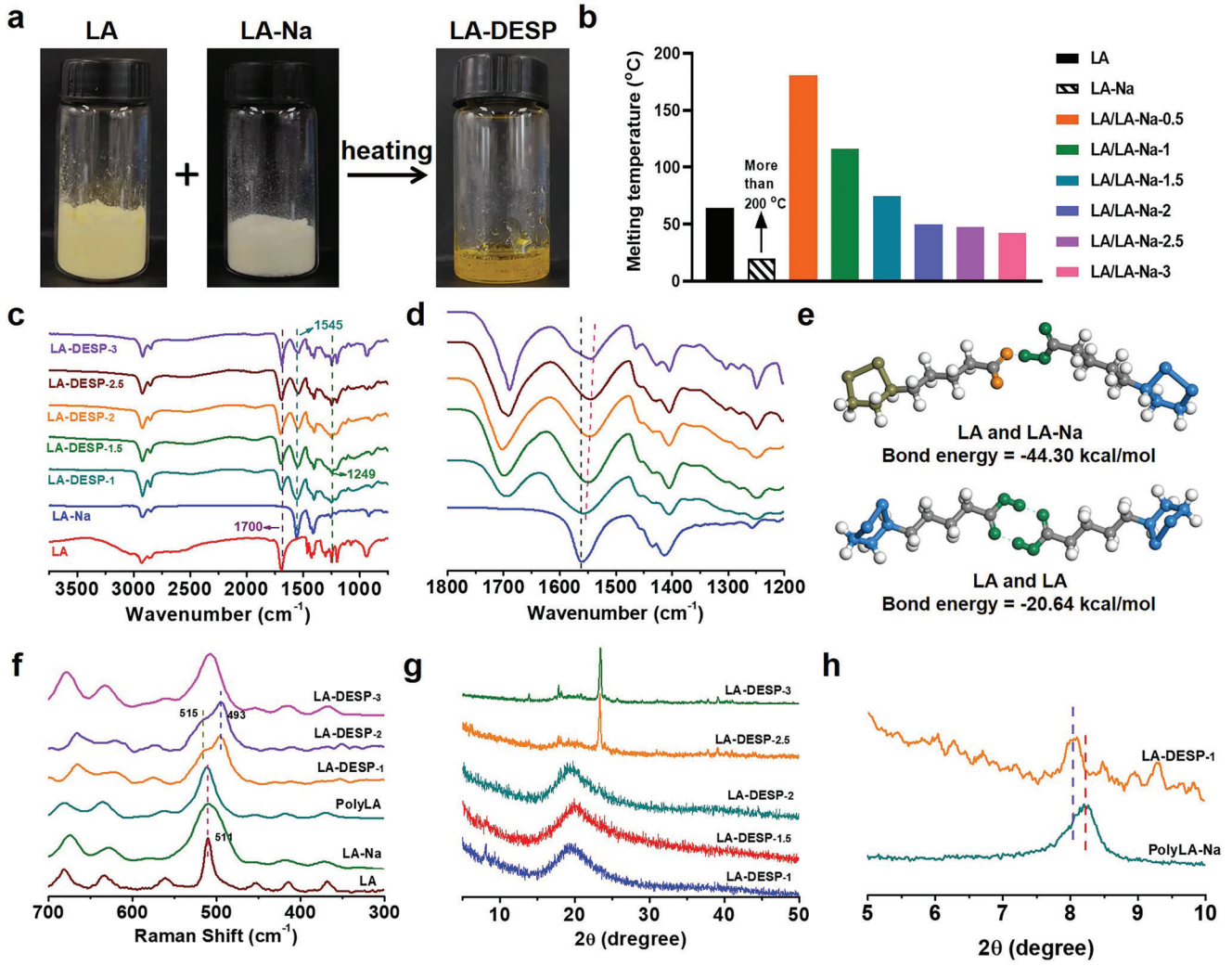

Figure 2. a) Preparation of LA-DESPs by heating LA and LA-Na mixture; b) Melting temperatures of LA, LA-Na, and mixtures of LA and LA-Na with different ratios tested by DSC; c) FT-IR spectra of the LA, LA-Na, and LA-DESPs with different ratios; d) Local magnification of FT-IR spectra of LA-Na and LA-DESPs with different ratios; e) Molecular dynamics simulation of bond energy of hydrogen bond formed between LA and LA-Na as well as LA dimer; f) Raman spectra of the LA powder, LA-Na powder, pure PolyLA, and LA-DESPs with different ratios; g) XRD patterns of LA-DESPs with different ratios; h) XRD spectra of polyLA-Na and LA-DSEPS$_{-1}$.

self-assembly of excessive polyLA-Na in the system.[29] With the increase of LA content in LA/LA-Na binary system, the intensity of diffraction peak of polyLA-Na gradually decreased and eventually disappeared, indicating formation of amorphous phase. In the binary system, the random copolymerization of LA and LA-Na as well as the —COOH…O═C—O$^-$ hydrogen bond interaction between LA and LA-Na led to the breakdown of the ordered layered self-assembly of polyLA-Na. Moreover, comparing the XRD results of the **LA-DESP**$_{-1}$ and the pristine polyLA-Na film reveals that the diffraction angle of polyLA-Na decreased after copolymerization with LA (Figure 2h), implying that polyLA increased the interlayer distances of polyLA-Na.[29] However, with the continued increase of the content of LA in the system, the sharp crystalline peaks of LA monomer (Figure S7, Supporting Information) appeared again in **LA-DESP**$_{-2.5}$ and **LA-DESP**$_{-3}$, further indicating that partial polyLA was metastable and depolymerized at room temperature.

2.2. Mechanical and Adhesive Properties of LA-DESPs

The mechanical properties of **LA-DESP**s were evaluated by tensile test. By adjusting the mass ratio of LA to LA-Na, the mechanical properties of **LA-DESP**s could be modulated over a large range. As mentioned above, the **LA-DESP**s experienced a transition from crystalline structure to amorphous structure and then to crystalline structure with the increase of LA content, so the tensile strength of **LA-DESP**s first decreased and then increased with the increment of LA content (**Figure 3**a), but the elongation was the opposite, due to the decrease of polymer chain mobility (Figure 3b). At a low LA content, the **LA-DESP** was brit-

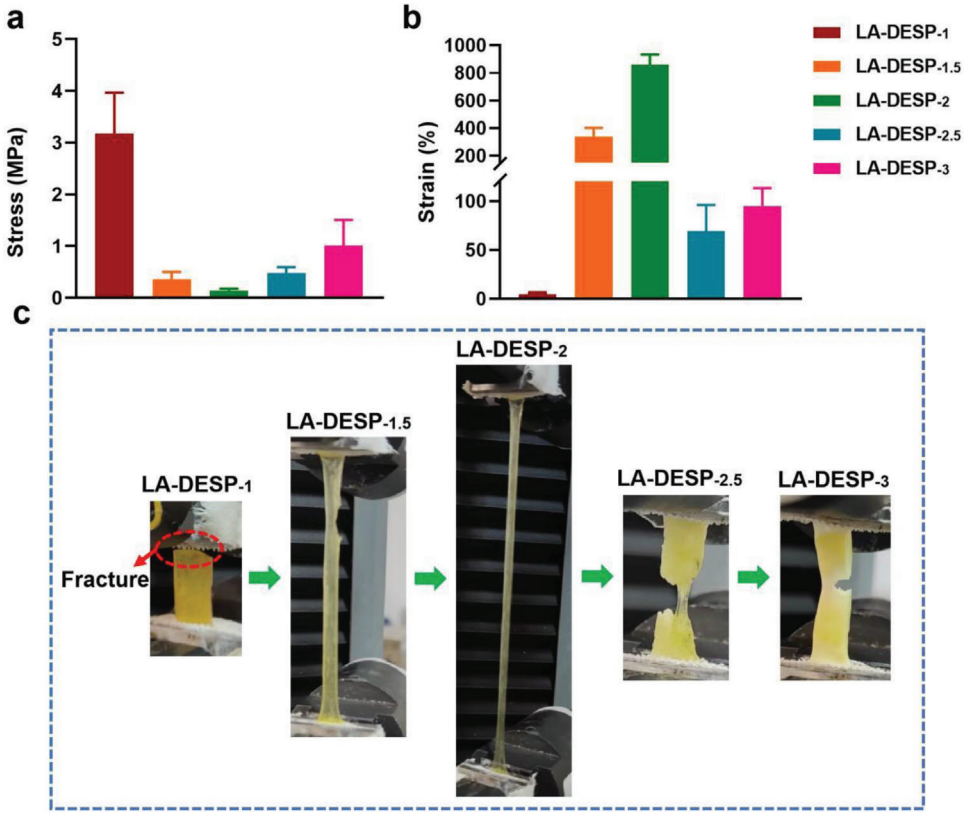

Figure 3. a) Tensile stress of LA-DESPs with different compositions ($n \geq 4$); b) Tensile strain of LA-DESPs with different compositions ($n \geq 4$); c) Pictures showing the stretching process of LA-DESPs with different compositions.

tle and rigid due to the existence of crystalline phase of polyLA-Na, and a high tensile strength (3.18 ± 0.7 MPa for **LA-DESP**$_{-1}$) and low elongation (4.7 ± 1.5% for **LA-DESP**$_{-1}$) were achieved. Upon increasing LA content, with gradual evolution from crystalline to amorphous structure, the **LA-DESP** became highly flexible and extensible owing to the formation of multiple dynamic hydrogen bonds between the polyLA and the polyLA-Na, which aided in energy dissipation (tensile strength was 0.14 ± 0.02 MPa and elongation was 860 ± 50% for **LA-DESP**$_{-2}$). Nevertheless, when LA/LA-Na was greater than 2, the **LA-DESP** changed into crystalline state again due to the reversible depolymerization of polyLA, so the tensile strength of **LA-DESP** was enhanced again, while the elongation declined (tensile strength was 1.01 ± 0.35 MPa and elongation was 95 ± 17% for **LA-DESP**$_{-3}$). The tensile stress–strain curves and macroscopic tensile behavior of **LA-DESP**s also reflected the transformation of the **LA-DESP**s from crystalline to amorphous state and then to crystalline state (Figure 3c; Figure S8, Supporting Information).

The tunable melting temperature, abundant adhesive carboxyl groups, and in situ curing ability after cooling made **LA-DESP** an excellent hot melt adhesive. The adhesion ability of **LA-DESP**s with different ratios to various substrates was investigated by lap shear test. As shown in **Figure 4**a–e and Figure S9 (Supporting Information), the adhesion strength of **LA-DESP**s to different substrates all showed a trend of decrease first and then increase, which was consistent with the variation trend of tensile strength of **LA-DESP**s, suggesting that the bulk strength of **LA-DESP**s played a key role in adhesion. Taking the iron sheet as an example, in the lap shear test, the adhesives exhibited a transition from interface failure to cohesion failure and then to interface failure with the increase of LA content (Figure S10, Supporting Information). Remarkably, the **LA-DESP**$_{-1}$ adhered-iron sheets with an adhesion area of 1.8 cm ×1 cm could easily lift a weight of 15 kg in the vertical direction and 1.25 kg in the horizontal direction, manifesting an excellent adhesion ability (Figure 4f). The above results revealed the crystal structure in the hot melt adhesive is of vital significance for enhancing the adhesion strength.

Next, the water-resistance adhesion capabilities of **LA-DESP** adhesives were examined by soaking the **LA-DESP**s-adhered iron sheets in water for different times (**Figure 5**a–f; Figure S11, Supporting Information). The results show that except for **LA-DESP**$_{-2}$, the adhesion strength of **LA-DESP**s with other proportions decreased obviously after soaking in water for 1 day compared with dry state; Especially, the **LA-DESP**$_{-1}$ suffered the most serious loss in adhesion strength. After soaking in water for 2 days, the adhesion strengths of **LA-DESP**$_{-1,}$ **LA-DESP**$_{-1.5,}$ **LA-DESP**$_{-2.5,}$ and **LA-DESP**$_{-3}$ to iron sheets were measured to be 53.9, 70.6, 333.3, and 450.9 kPa, respectively. Further extending the soaking time in water to 3 days, the adhesion strengths of these adhesives to iron sheet could only keep 35.3, 31.7, 32.4, and 71.9 kPa, respectively. However, unexpectedly, the adhesion strength of **LA-DESP**$_{-2}$ increased significantly after immersion in water compared with its dry state. After soaking in water for 1 day, the adhesion strength of **LA-DESP**$_{-2}$ increased from 137 kPa

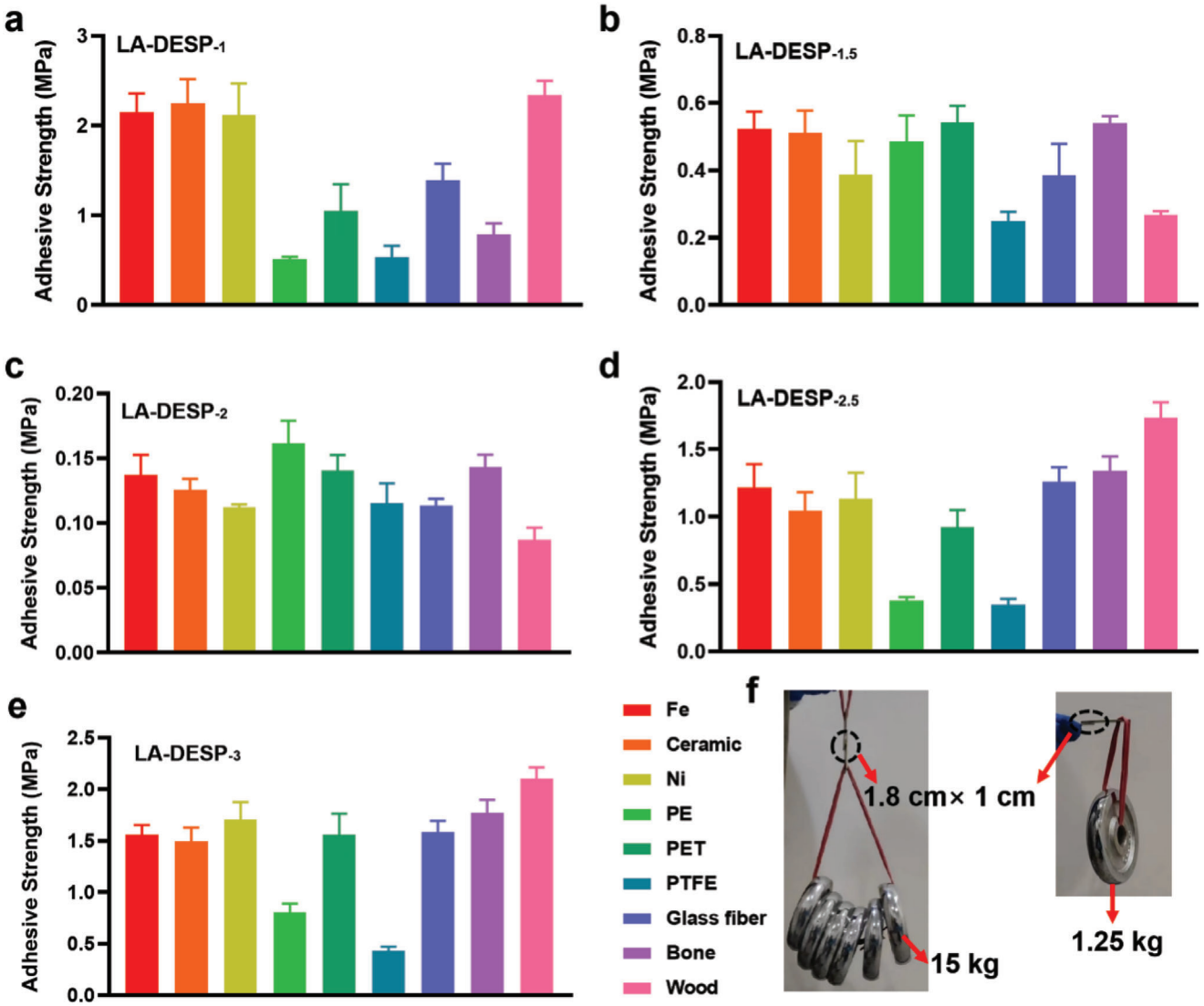

Figure 4. a–e) Adhesion strength of LA-DESPs with different ratios ($n \geq 4$); f) Digital images depicting the ability of the LA-DESP$_{-1}$-bonded-iron sheets (adhesion area: 1.8 cm × 1 cm) to lift 15 kg weight in the vertical direction and 1.25 kg weight in the horizontal direction.

in dry state to 1.07 MPa. Although the adhesion strength gradually decreased with the extension of immersion time in water, it was still higher than that in dry state even after soaking in water for 4 days (465 kPa). The emerging unique adhesion characteristic of **LA-DESP**s in water was supposedly originated from the change of network structure of the adhesive caused by water molecules. In order to verify this, we employed XRD to investigate the structure changes of **LA-DESP**s that were adhered to iron sheets and then soaked in water for different times (Figures S12–S15, Supporting Information). As presented in Figure 5g, hydration led to a decrease in bulk strength of **LA-DESP**$_{-1}$ and **LA-DESP**$_{-1.5}$ due to entry of water molecules into the hydrophilic 2D channel formed by polyLA-Na.[29] Correspondingly, both of the adhesives changed from interface failure in dry state to cohesion failure in the process of lap shear, so the adhesion strength was sacrificed significantly. However, for the **LA-DESP**$_{-2.5}$ and **LA-DESP**$_{-3}$, the polyLA was further depolymerized into lower molecular weight oligomers after contacting with water. In this condition, the bulk of the adhesive was easily destroyed when stretched, since the entry of water molecules resulted in the dissociation of —COOH…O=C—O$^-$ hydrogen bond between polyLA and polyLA-Na, thus reducing the ability of polyLA-Na stabilize polyLA. Interestingly, the **LA-DESP**$_{-2}$ changed from amorphous to crystalline structure after contact with water, and a sharp crystallization peak of LA monomer appeared in **LA-DESP**$_{-2}$, implying that partial polyLA was depolymerized. The appearance of crystalline structure enhanced the bulk strength of **LA-DESP**$_{-2}$, which in turn contributed to the increase of adhesion strength. It is clearly depicted that the adhesive transformed from cohesion failure in dry state to interface failure in the process of lap shear (Figure 5g). With the extension of immersion time in water, the adhesion strength of **LA-DESP**$_{-2}$ decreased because the entry of excess water molecules further increased the depolymerization of polyLA, resulting in a dramatic reduction in the bulk strength

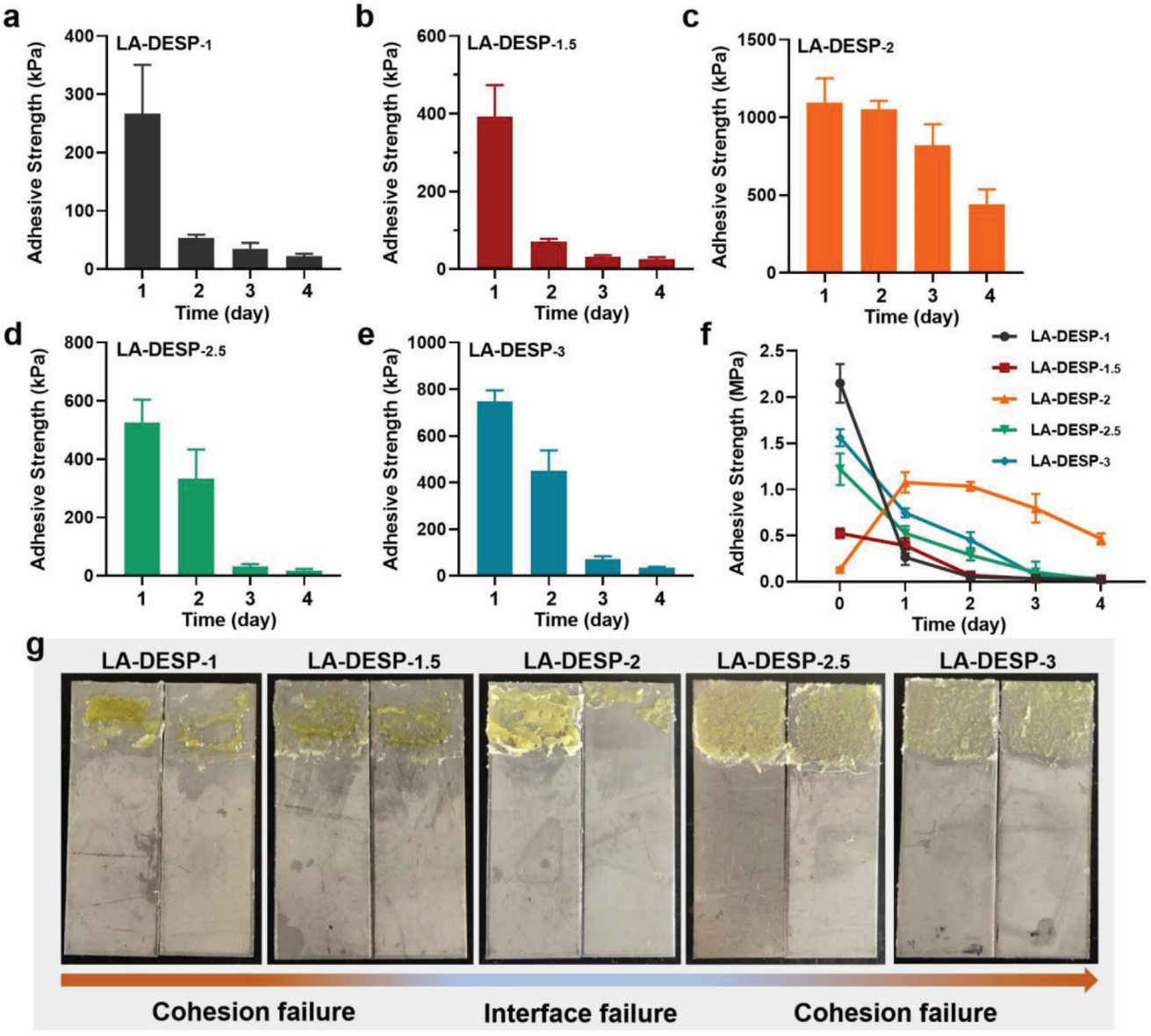

Figure 5. a–e) Adhesion strength of LA-DESPs to iron sheets after soaking in water for different times; f) Variation trend of adhesion strength of LA-DESPs after soaking in water for different times. g) LA-DESPs show adhesive damage from cohesion failure to interface failure and then to cohesion failure in the lap shear test after soaking in water for 2 days.

of the adhesive. Similar phenomenon also occurred to the **LA-DESP**$_{-2.5}$ and **LA-DESP**$_{-3}$.

Considering the appropriate melting temperature and structural stability, **LA-DESP**$_{-2}$ was chosen as a tissue adhesive, and its tissue adhesion strength at 37 °C was investigated by lap shear test. **Figure 6**a and Figure S16a (Supporting Information) show that the adhesion strengths of **LA-DESP**$_{-2}$ to pig skin, stomach, and muscle at 37 °C could reach 57.1, 38.2, and 25.5 kPa, respectively. Then, we placed the adhered pig skin in water for different times to investigate its water resistance adhesion to tissue at 37 °C (Figure 6b; Figure S16b, Supporting Information). With the increase of soaking time, the adhesion strength of **LA-DESP**$_{-2}$ to pig skin decreased gradually, but could still maintain 22 kPa after soaking in water for 12 h at 37 °C. As analyzed above, the decrease of the adhesion strength was caused by the depolymerization of polyLA in water. Nonetheless, the above results manifest that **LA-DESP**$_{-2}$ possesses a lasting underwater adhesion ability to tissue.

In order to investigate the effect of the configuration of LA on the deep eutectic, we studied the deep eutectic behavior of the mixture of LA and LA-Na with R-isomer (LA-R) and racemic (LA-Ra) structure. Intriguingly, the LA/LA-Na mixture of the R-isomer and racemic structure showed a similar deep eutectic phenomenon to that of S-isomer LA/LA-Na mixture. With the increase of LA content in the mixture, the melting point of the mixture decreases continuously. When LA/LA-Na $\geq$ 2, the melting temperature of the mixture is obviously lower than that of pure LA and LA-Na, which indicates that the deep eutectic behavior of lipoic acid and its salts mixture is universal and independent of

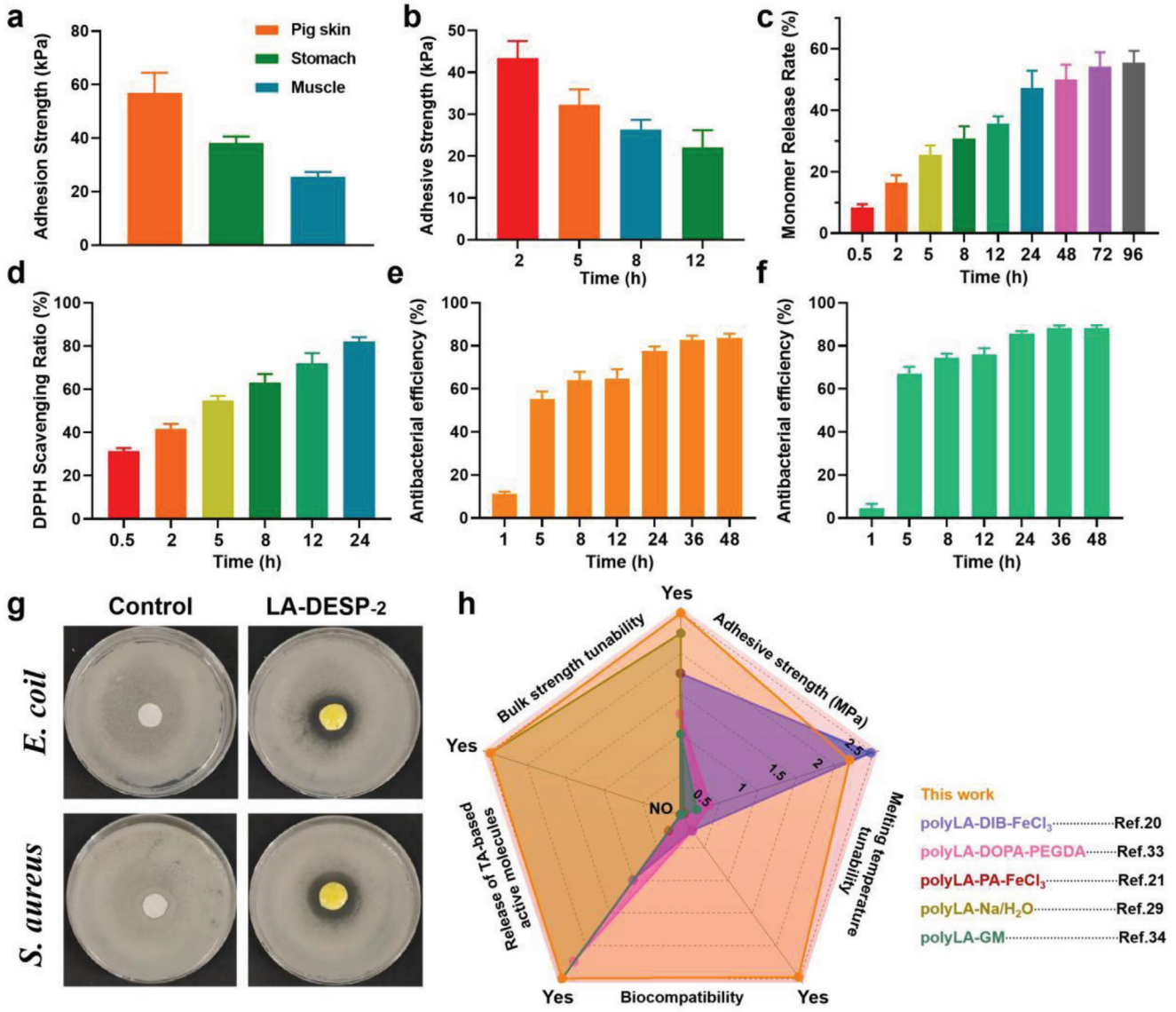

Figure 6. a) Adhesion strength of LA-DESP$_{-2}$ to pig skin, stomach, and muscle at 37 °C ($n \geq 4$); b) Adhesion strengths of LA-DESP$_{-2}$ adhered to pig skin after soaking in water for different time periods ($n \geq 4$); c) Monomer release ratio of LA-DESP$_{-2}$ in PBS for different times ($n = 3$); d) DPPH radical clearance ratio of LA-DESP$_{-2}$ determined at different times ($n = 3$); e) Sterilization rate of LA-DESP$_{-2}$ against *E. coli* at different times ($n = 3$); f) Sterilization rate of LA-DESP$_{-2}$ against *S. aureus* at different times ($n = 3$); g) Digital images displaying representative inhibition zone results for LA-DESP$_{-2}$ against *E. coli* and *S. aureus* at 24 h; h) Comprehensive performance of the LA-DESPs compared to other LA-based materials reported in the literature.

lipoic acid configuration (Figures S17 and S18, Supporting Information). Next, we used LA/LA-Na mixtures of the racemic and R-isomer structure as deep eutectic supramolecular adhesives to investigate their adhesion properties. Using iron sheet and ceramic as the adhesion substrates, we found that for LA-Ra-based adhesive, the adhesion trend is consistent with that of S-isomer LA-based adhesive. With the increase of LA-Ra content, the adhesion strength decreases at first and then increases, and when LA-Ra/LA-Na-Ra is 2, the adhesion strength is the lowest. That is because with the increase of LA, the polymer in the adhesive changes from crystallization to amorphous and then to crystallization, which makes the bulk strength of the adhesive decrease at first and then increase (Figure S19, Supporting Information). For LA-R-based adhesive, it also shows excellent adhesion, and the adhesion strength also decreases first and then increases with the increment of LA-R content. However, the adhesion strength of the LA-R-based adhesive is the lowest when LA-R/LA-Na-R is 2.5, which is not consistent with the racemic and S-isomer LA-based hot melting adhesives (Figure S20, Supporting Information). The reason may be the change of the crystallization behavior of the copolymer in the adhesive due to the different configuration of lipoic acid. To sum up, the deep eutectic behavior of the mixture of lipoic acid and its salt is universal and independent of its configuration, and these mixtures can all be used to prepare hot melt adhesives and show satisfactory adhesion properties.

2.3. In Vitro Bioactivity of LA-DESP

LA has been proved to possess an excellent antioxidant and anti-bacterial function.[11–13] However, few of the LA-based materials reported so far have harnessed its bioactive function, since LA monomer is not easily released out in an aqueous environment due to its hydrophobic nature, so the biological activity of LA is greatly sacrificed.[21–23] In contrast to this, LA-Na is an amphiphilic molecule with excellent water solubility. Rapid dissociation of polyLA-Na in aqueous solution can effectively release small LA-Na bioactive molecules. However, the too fast dissociation rate of pristine polyLA-Na (20 min) is not suitable for application in vivo.[29] In this work, we discovered that the combination of polyLA and polyLA-Na could reduce the dissociation rate of the polyLA-Na and realize the slow and sustainable release of LA-Na by forming multiple —COOH...O═C—O⁻ hydrogen bonds between polyLA and polyLA-Na. The LA-based monomer release rate of **LA-DESP**$_{-2}$ in PBS was inspected via UV–vis spectroscopy. As presented in Figure S21a (Supporting Information), the characteristic absorption peak intensity of the disulfide five-membered ring at 330 nm increased gradually with the immersion time in PBS, and no abrupt release was observed within a short period of time. We calculated the release efficiencies of monomers from **LA-DESP**$_{-2}$ (Figure 6c). The **LA-DESP**$_{-2}$ was shown to continuously release LA-based antioxidant monomers within 96 h (the release efficiency of LA-based monomers could reach 55.5% at 96 h). The monomer release efficiency of **LA-DESP**s with different compositions after soaking in PBS for 24 and 72 h was also tested. As shown in Figure S22 (Supporting Information), the monomer release efficiency of **LA-DESP**s is significantly higher than that of pure PolyLA, because the hydrophobicity of LA limits the release of LA in PolyLA in aqueous environment. Moreover, the monomer release efficiency of **LA-DESP**s decreases with the increase of LA content, which indicates that the released monomer is mainly in the form of LA-Na, and the introduction of LA-Na into **LA-DESP**s can significantly improve the release efficiency of LA-based bioactive molecules. This proves that the combination of polyLA and polyLA-Na could effectively restrain the dissociation rate of polyLA-Na.

In light of the excellent antioxidant capacity of LA-based monomers,[11–13] the antioxidant effect of the **LA-DESP**$_{-2}$ on 1,1-diphenyl-2-picrylhydrazyl free radical (DPPH) was detected to evaluate the ROS scavenging activity according to the previously reported protocol.[31,32] As shown in Figure 6d and Figure S21b (Supporting Information), the **LA-DESP**$_{-2}$ exhibited a high DPPH clearance efficiency and could achieve 82% scavenging activity after 24 h. Figure S21c (Supporting Information) exhibits the results of naked-eye observation on the decolorization reaction of DPPH reagent with PBS or **LA-DESP**$_{-2}$. After 24 h of incubation, the dark purple color of the DPPH solution turned yellow, demonstrating the decolorization of DPPH radicals in the presence of **LA-DESP**$_{-2}$. Whereas no decolorization occurred after PBS treatment. The macroscopic color change reflects intuitively the enhanced ROS scavenging activity with the monomer release of the LA-Na from the **LA-DESP**$_{-2}$.

In addition to excellent antioxidant activity, LA-based monomer has also been shown to possess an antibacterial activity against both Gram-negative and Gram-positive bacteria through increasing the permeability of bacterial cell membrane.[24,25] In this experiment, we observed bacterial proliferation of *E. coil* and *S. aureus* co-cultured with **LA-DESP**$_{-2}$. As shown in Figure 6e,f and Figure S23 (Supporting Information), with the extension of co-culture time, the antibacterial efficiency increased gradually. When the co-culture time was extended to 48 h, the antibacterial efficiency of **LA-DESP**$_{-2}$ to *E. coil* and *S. aureus* was 83% and 88%, respectively. Moreover, there was an obvious inhibition zone after co-culture of **LA-DESP**$_{-2}$ and bacteria, which once again corroborated that **LA-DESP**$_{-2}$ had an excellent antibacterial ability (Figure 6g). To sum up, the **LA-DESP** adhesives not only circumvent the drawbacks of traditional LA-based materials that need to introduce other exogenous substances to stabilize, but also demonstrate tunable melting temperature, high adhesion, sustainable release of LA-based active molecules, and excellent biological activity. In comparison, the comprehensive performances of LA-based materials previously reported in the literature are summarized in Figure 6h.[20,21,29,33,34] Although the adhesion strength of polyLA-DIB-$FeCl_3$ hot melting adhesive was slightly higher than that of **LA-DESP**s, its application in the field of biomedicine might be limited by its higher melting temperature, the potential toxicity of small molecules and the inability to release LA-based active molecules.[20] Therefore, based on its robust adhesion at physiological temperature, and bioactivity, we developed **LA-DESP**s as a tissue adhesive to replace surgical suture to accelerate the healing of injured tissue in this study.

2.4. Biocompatibility and In Vivo Application of LA-DESP

As a bioadhesive, besides excellent tissue adhesion and bioactivity, biocompatibility is also a prerequisite that decide it's in vivo application for tissue repair. Moreover, an ideal tissue adhesive should induce no or little hemolysis upon contacting bleeding damaged tissue. Thus, we first evaluated the hemocompatibility of **LA-DESP**$_{-2}$. **Figure 7**a shows photographs of whole blood centrifuge supernatant treated with different mass concentrations of **LA-DESP**$_{-2}$, phosphate buffered saline (PBS) negative group, and deionized water positive group. The **LA-DESP**$_{-2}$ groups were all transparent bright yellow similar to negative group, while positive group was bright red. The hemolysis ratios of **LA-DESP**$_{-2}$ with different mass concentrations were all <5% (Figure 7b), which was considered as the safe level for tissue adhesive. Then, we assayed the cytocompatibility of the **LA-DESP**$_{-2}$. The cytotoxicity was evaluated by co-culturing L929 cells with the different mass concentrations of **LA-DESP**$_{-2}$. As shown in Figure S24 (Supporting Information), the cells spread evenly and survived well, as indicated by observing rich green fluorescent spots in the fluorescent image obtained by live/dead assay in two mass concentrations of **LA-EDSP**$_{-2}$ samples (10 and 20 μg ml^{-1}). The cell activity was quantitatively evaluated by MTT assay (Figure 7c). It is seen that these two concentrations of **LA-EDSP**$_{-2}$ samples showed comparable cell viability with the control group after co-culturing with cells for 1 and 3 days. In order to ensure that the **LA-DESP**$_{-2}$ will not cause cytotoxicity to the organism when used in vivo, we detected the plasma concentration of LA-based molecule in rats at different times by implanting the **LA-DESP**$_{-2}$ under the skin of the back of the rat. The results show that the highest plasma con-

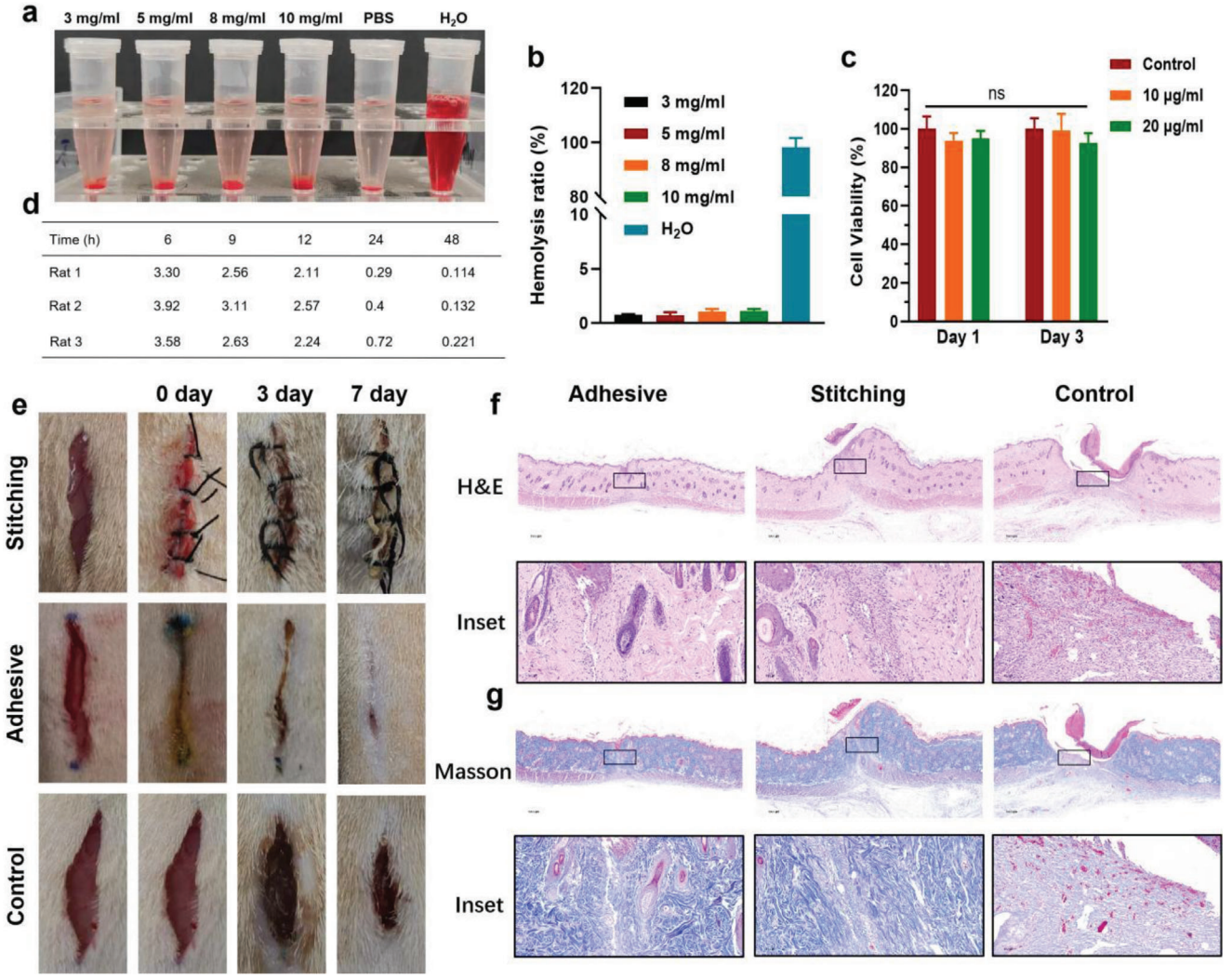

Figure 7. a,b) Hemocompatibility of LA-DESP$_{-2}$ with different mass concentration (3–10 mg ml^{-1}); c) Cell viability of L929 cells co-cultured with LA-DESP$_{-2}$ for 1 and 3 days($n \geq 4$); d) In vivo plasma concentration of LA-based molecule at different times after implantation of LA-DESP$_{-2}$ under the skin of back of rats (the unit of the plasma concentration was μg ml^{-1}); e) Photographs of the rat incised skin after treatments with different methods; f) H&E staining and g) Masson staining of the wound sites on day 7 ($n = 3$ biologically independent samples in each group).

centration was 3.92 μg mL^{-1} after the **LA-DESP$_{-2}$** was implanted under the skin of rat for 3 h, which was much lower than the minimum concentration (10 μg mL^{-1}) used in vitro cytocompatibility test, at which cell maintained a high viability (Figure 7d). In addition, the histocompatibility of **LA-DESP$_{-2}$** in vivo was also evaluated by subcutaneous implantation. The H&E staining results show that compared with the normal tissue, there was no significant inflammation, necrosis, or metaplasia for the subcutaneous tissue treated with the **LA-DESP$_{-2}$** for 2 days (Figure S25, Supporting Information), indicating that **LA-DESP$_{-2}$** stimulated no acute reaction for subcutaneous mucosal tissue. Histological assessment of major organs including the heart, liver, spleen, lung, and kidney reveals that the **LA-DESP$_{-2}$** did not cause any damage to these organs (Figure S25, Supporting Information). These data prove that **the LA-DESP$_{-2}$** did not cause local or systemic toxicity to rats, showing excellent biosafety and biocompatibility.

Considering its rapid tissue sealing ability, release behavior of bioactive molecules, and reliable biocompatibility, **LA-DESP$_{-2}$** was used as tissue adhesive to replace surgical sutures to accelerate skin wound healing in rat model. The animal experiments are carried out with reference to the works currently reported.[35,36] Before the operation, the **LA-DESP$_{-2}$** was heated to 49 °C in a syringe, and after it was completely melted, the temperature was reduced to 45 °C, and then the molten **LA-DESP$_{-2}$** was quickly extruded to the skin wound of the rat. **LA-DESP$_{-2}$** was quickly cooled down to body temperature and solidified in situ at the wound to achieve firm adhesion to the wet wound tissue. Although the surgical suture could also close the wound, an obvious secondary damage to the surrounding tissue was observed (Figure 7e). After **LA-DESP$_{-2}$** treatment for 3 days the incised wound was tightly sealed, and the treatment time was prolonged to 7 days, the wound was almost completely closed. As for suture group, the skin incision was well-bridged but the sutures remained in the skin interface hindered tissue regeneration. Whereas for the con-

trol group, the skin wound showed infection and there was still significant injury on the seventh day. The above results demonstrate that the **LA-DESP**$_{-2}$ bioglue could considerably promote skin wound healing.

H&E staining reveals that after **LA-DESP**$_{-2}$ treatment for 7 d, the epidermis was completely regenerated, and there were evident hair follicles and sebaceous glands near the incision. Whereas an apparent unrecovered dermis was observed in the wounds of the control on day 7. The healing in the suture group was relatively better, but the healing surface was uneven (Figure 7f). Masson trichrome staining showed that the collagen arrangement of **LA-DESP**$_{-2}$-treated wounds was more similar to that of normal skin, and epidermal regeneration was more complete than that of control and suture-treated groups on day 7 (Figure 7g). These in vivo results indicated that the **LA-DESP**$_{-2}$ bioglue accelerated wound closure and tissue regeneration. All animal experiments were approved by the Institutional Animal Care and Use Committee of Yi Shengyuan Gene Technology (Tianjin) Co., Ltd. (Approval NO. YSY-DWLL-2023151).

3. Conclusion

In this work, a deep eutectic effect was discovered in the mixture of α-lipoic acid (LA), a coenzyme, and its coenzyme salt, sodium α-lipoic acid (LA-Na). This unexploited mechanism was harnessed for the first time to create deep eutectic supramolecular polymer (**LA-DESP**) adhesives by simple one-step heating of a mixture of LA and LA-Na. The multiple —COOH...O═C—O$^-$ hydrogen bond interactions between LA and LA-Na were shown to significantly reduce the melting temperature of the mixture and modulate the melting temperature to near body and pathological temperature by just adjusting the ratio of LA to LA-Na, which greatly increasing the in vivo application possibility of LA-based polymers. In addition, the random copolymerization of LA and LA-Na could effectively quench the sulfur-free radicals at the end of polyLA and the strong hydrogen bonds between polyLA and polyL-Na could contribute to the formation of stable **LA-DESP** at room temperature without introducing any exogenous small molecule or ion stabilizing agents. Importantly, the **LA-DESP** could effectively and sustainably release LA-based active molecules and show satisfactory antioxidant and antibacterial activity. Remarkably, the in-situ curing property of **LA-DESP** and rich adhesive carboxyl groups allowed for fast and high-strength adhesion to a variety of substrates, including wet tissues. The **LA-DESP**-adhered tissue could keep stable bond under water for a long time at 37 °C. Furthermore, in vitro and in vivo assays confirmed the better biocompatibility of **LA-DESP**. The **LA-DESP** was explored as a surgical suture to seal the damaged skin tissue of rats. Post-surgical outcome demonstrated that the **LA-DESP** adhesive could firmly adhere to wet wound tissue and significantly accelerate wound healing. We anticipate that this study will provide a novel option to develop bioadhesives in the future by exploiting deep eutectic effect undiscovered and existing in other naturally bioactive molecules.

Supporting Information

Supporting Information is available from the Wiley Online Library or from the author.

Acknowledgements

The authors gratefully acknowledge the support for this work from the National Natural Science Foundation of China (Grant No. 52233008 and 51733006).

Conflict of Interest

The authors declare no conflict of interest.

Data Availability Statement

The data that support the findings of this study are available in the supplementary material of this article.

Keywords

deep eutectic, supramolecular polymer adhesives, tissue adhesion, wound healing, α-lipoic acid

Received: July 3, 2023
Published online: July 19, 2023

[1] P. Q. Yao, Q. W. Bao, Y. Yao, M. Xiao, Z. Y. Xu, J. H. Yang, W. G. Liu, *Adv. Mater.* **2023**, *35*, 2300114.
[2] Y. C. Wan, S. S. Huang, Y. X. Sun, H. Zhu, Q. B. Zheng, Q. Zhang, S. P. Zhu, *Chem. Eng. J.* **2022**, *442*, 136289.
[3] B. Yiming, Y. Han, Z. L. Han, X. N. Zhang, Y. Li, W. Z. Lian, M. Q. Zhang, J. Yin, T. L. Sun, Z. L. Wu, T. F. Li, J. Z. Fu, Z. Jia, S. X. Qu, *Adv. Mater.* **2021**, *33*, 2006111.
[4] Y. Zhang, Y. F. Wang, Y. Guan, Y. J. Zhang, *Nat. Commun.* **2022**, *13*, 6671.
[5] G. Ge, K. Mandal, R. Haghniaz, M. Li, X.i. Xiao, L. Carlson, V. Jucaud, M. R. Dokmeci, G. W. Ho, A. Khademhosseini, *Adv. Funct. Mater.* **2023**, *33*, 2207388.
[6] Y. J. Liang, K. F. Wang, J. J. Li, Y. F. Zhang, J. P. Liu, K. H. Zhang, Y. H. Cui, M. K. Wang, C. S. Liu, *Mater. Horiz.* **2022**, *9*, 1700.
[7] C. Vidal, J. G. Ivarez, A. H. Gmez, A. R. Kennedy, E. Hevia, *Angew. Chem., Int. Ed.* **2014**, *53*, 5969.
[8] E. L. Smith, A. P. Abbott, K. S. Ryder, *Chem. Rev.* **2014**, *114*, 11060.
[9] X. Ge, C. D. Gu, X. L. Wang, J. P. Tu, *J. Mater. Chem. A* **2017**, *5*, 8209.
[10] S. G. Wu, C. Y. Cai, F. F. Li, Z. J. Tan, S. Y. Dong, *Angew. Chem., Int. Ed.* **2020**, *59*, 11871.
[11] S. Y. Lv, S. S. He, X. L. Ling, Y. Q. Wang, C. Huang, J. R. Long, J. Q. Wang, Y. Qin, H. Wei, C. Y. Yu, *Int. J. Pharm.* **2022**, *267*, 122201.
[12] P. Jing, Y. L. Luo, Y. Chen, J. B. Tan, C. Y. Liao, S. Y. Zhang, *Bioconjugate Chem.* **2023**, *34*, 366.
[13] L. Wang, P. Jing, J. Tan, C. Y. Liao, Y. Chen, Y. L. Yu, S. Y. Zhang, *Biomaterials* **2021**, *273*, 120823.
[14] W. T. Li, J. R. Peng, Q. Yang, L. J. Chen, L. Zhang, X. X. Chen, Z. Y. Qian, *Biomater. Sci.* **2018**, *6*, 1201.
[15] M. Li, L. B. Ling, Q. Xia, X. S. Li, *RSC Adv.* **2021**, *11*, 12757.
[16] Z. Z. Wu, P. F. Zhang, P. W. Wang, Z. Z. Wang, X. L. Luo, *Nanoscale* **2021**, *13*, 3723.
[17] F. H. Meng, R. Cheng, C. Deng, Z. Y. Zhong, *Mater. Today* **2012**, *15*, 436.
[18] X. Y. Zhang, R. M. Waymouth, *J. Am. Chem. Soc.* **2017**, *139*, 3822.
[19] C. Chen, X. Yang, S. J. Li, C. Zhang, Y. N. Ma, Y. X. Ma, P. Gao, S.-Z. Gao, X. J. Huang, *Green Chem.* **2021**, *23*, 1794.
[20] Q. Zhang, C. Y. Shi, D. H. Qu, Y. T. Long, B. L. Feringa, H. Tian, *Sci. Adv.* **2018**, *4*, eaat8192.

[21] A. Khan, R. R. Kisannagar, C. Gouda, D. Guptab, H. C. Lin, *J. Mater. Chem. A* **2020**, *8*, 19954.
[22] Y. J. Wang, S. T. Sun, P. Y. Wu, *Adv. Funct. Mater.* **2021**, *31*, 2101494.
[23] Q. Zhang, Y. X. Deng, C. Y. Shi, B. L. Feringa, H. Tian, D. H. Qu, *Matter* **2021**, *4*, 1352.
[24] W. Y. Zhou, Y. W. Du, X. S. Li, C. Yao, *Med. Chem.* **2020**, *28*, 115682.
[25] C. Shi, Y. Sun, X. R. Zhang, Z. W. Zheng, M. C. Yang, H. Ben, K. K. Song, Y. F. Cao, Y. F. Chen, X. Liu, R. Dong, X. D. Xia, *Food Control* **2016**, *59*, 352.
[26] C. Y. Cui, B. Liu, T.e. L. Wu, Y. Liu, C. C. Fan, Z. Y. Xu, Y. Yao, W. G. Lui, *J. Mater. Chem. A* **2022**, *10*, 1257.
[27] J. I. Taka, S. Ogino, S. Kashina, *Acta Crystallogr.* **1998**, *54*, 384.
[28] L. DAscenzo, P. Auffinger, *Acta Crystallogr.* **2015**, *71*, 164.
[29] Q. Zhang, Y. X. Deng, H. X. Luo, C. Y. Shi, G. M. Geise, B. L. Feringa, H. Tian, D. H. Qu, *J. Am. Chem. Soc.* **2019**, *141*, 12804.
[30] C. Dang, M. Wang, J. Yu, Y. Chen, S. H. Zhou, X. Feng, D. T. Liu, H. S. Qi, *Adv. Funct. Mater.* **2019**, *29*, 1902467.
[31] Y. Liu, R. Guo, T. L. Wu, Y. N. Lyu, M. Xiao, B. B. He, G. W. Fan, J. H. Yang, W. G. Liu, *Chem. Eng. J.* **2021**, *418*, 129352.
[32] Y. Liu, X. P. Zhang, T. L. Wu, B. Liu, J. H. Yang, W. G. Liu, *Nano Today* **2021**, *41*, 101306.
[33] J. Y. Chen, D. W. Guo, S. H. Liang, Z. Z. Liu, *Polym. Chem.* **2020**, *11*, 6670.
[34] Y. M. Gao, X. Zhan, S. H. Huo, L. Fu, Z. Tang, K. K. Qi, C. C. Lv, C. Y. Liu, Y. L. Zhu, S. G. Ding, Y. M. Lv, *J. Mater. Chem. B* **2022**, *10*, 2171.
[35] Z. L. Wang, X. Q. Gu, B. Li, J. J. Li, F. Wang, J. Sun, H. J. Zhang, K. Liu, W. S. Guo, *Adv. Mater.* **2022**, *34*, 2204590.
[36] C. Ma, J. Sun, B. Li, Y. Feng, Y. Sun, L. Xiang, B. H. Wu, L. L. Xiao, B. M. Liu, V. S. Petrovskii, B. Liu, J. R. Zhang, Z. L. Wang, H. Y. Li, L. Zhang, J. J. Li, F. Wang, R. Göstl, I. I. Potemkin, D. Chen, H. B. Zeng, H. J. Zhang, K. Liu, A. Herrmann, *Nat. Commun.* **2021**, *12*, 3613.